

Influence of the Measurement Volume on the Phase Error in Phase Doppler Anemometry

Part 1: Reflective Mode Operation

Heinz-E. Albrecht*, Michael Borys**, Marcus Wenzel**, Thomas Wriedt***

(Received: 29 April 1993; resubmitted: 23 March 1994)

Abstract

In phase Doppler anemometry (PDA), phase difference errors are caused by the Gaussian intensity distribution of the laser beam and the curvature of the phase fronts outside of the beam waist. This results in erroneous particle sizes. Based on a physical analysis by geometrical optics [1], this phase difference error is

evaluated for reflected mode operation (Part I) and for refracted mode operation (Part II). By varying the particle trajectories statistically, the error in determining the particle size and the mass flow can be simulated. By the method described the error in the measured phase difference can easily be estimated.

1 Theoretical Foundations

Laser-based methods for measuring simultaneously the velocity and the size of moving particles have become a powerful tool in the investigation of multi-phase flows [2]. Many sizing methods are based on single particle scattering. Phase Doppler anemometry, which is based on laser Doppler anemometry (LDA), is finding a wide range of applications in research and development and has been extensively developed during the last decade [3-7].

In phase Doppler anemometry, the photodetectors are commonly placed at such angular positions that either only the reflected or the refracted component of the scattered light is the dominant component to be detected. In such cases relatively simple relationships between measured phase difference and particle size have been deduced [4-7]. They are valid for a particle situated at the centre of the measurement volume, scattering a plane wave. This means that the laser beam, which usually has a Gaussian-shaped intensity distribution, is approximated by a plane wave-front having constant intensity.

However, even a particle trajectory on the *x*-axis (Figure 1) through the centre of the measurement volume leads to measured phase difference errors which are dependent on the local position of the particle, if the signal generating points on the particle are outside of the plane wave-front region [8]. However, essentially for phase difference errors are the Gaussian distribution of the intensity and the curvature of the phase fronts beyond the beam waist.

In this paper, the phase difference errors which are dependent on the influence of the measurement volume for a phase Dop-

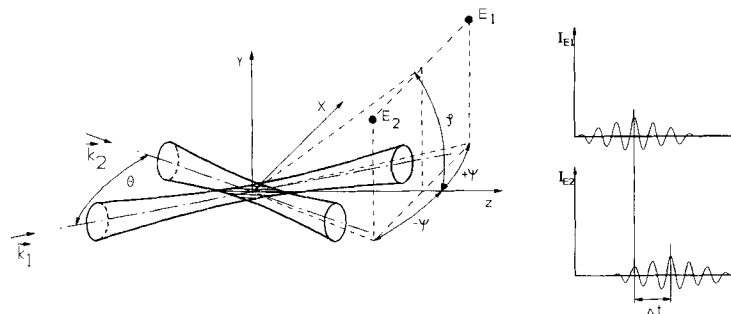


Fig. 1: Beam and receiver arrangement of the PDA.

pler anemometer operating in the reflective mode will be analysed. This means that the detectors (Figure 1) are situated at a position vector \vec{r}_{oe} relative to the centre of the measurement volume such that the reflected light component is dominant. The position vector is described by the radial distance r_0 , the off-axis-angle φ_0 and the elevation angle ψ_0 , with an index *e* denoting detector one or two:

$$\vec{r}_{oe} = r_0 \begin{pmatrix} \pm \sin \psi_0 \\ \cos \psi_0 \sin \varphi_0 \\ \cos \psi_0 \cos \varphi_0 \end{pmatrix} \quad e = 1, 2 \quad (1)$$

The two laser beams which form the measurement volume have a direction vector \vec{e}_{ks} :

$$\vec{e}_{ks} = \begin{pmatrix} \sin(\pm \theta/2) \\ 0 \\ \cos(\pm \theta/2) \end{pmatrix} \quad s = 1, 2 \quad (2)$$

The particle crossing the measurement volume has a velocity $\vec{v} = (v_x, v_y, v_z)^T$ and its local position is given by the vector \vec{r}_p :

$$\vec{r}_p = \begin{pmatrix} x_p \\ y_p \\ z_p \end{pmatrix} = \begin{pmatrix} x_0 + v_x t \\ y_0 + v_y t \\ z_0 + v_z t \end{pmatrix} \quad (3)$$

* Prof. Dr.-Ing. H.-E. Albrecht, Techno Trans e.V., Carl-Hopp-Straße 19 a, D-18069 Rostock (Federal Republic of Germany).

** Dipl.-Ing. M. Borys, Dipl.-Ing. M. Wenzel, Universität Rostock, Fachbereich Elektrotechnik, Institut für Allgemeine Elektrotechnik, Albert-Einstein-Straße 2, D-18051 Rostock (Federal Republic of Germany).

*** Dr.-Ing. T. Wriedt, Institut für Werkstofftechnik, Badgasteiner Straße 3, D-28334 Bremen (Federal Republic of Germany).

The trajectory of the particle is at its shortest distance from the centre of the coordinate system at a position of $\vec{r}_0 = (x_0, y_0, z_0)^T$ (Figure 2). From the given direction of the laser beams, the given position of the detectors and the law of reflection on a sphere [1]

$$\frac{\vec{e}_{pse} - \vec{e}_{ks}}{|\vec{e}_{pse} - \vec{e}_{ks}|} = \vec{e}_{rse} = \begin{pmatrix} x_{rse} \\ y_{rse} \\ z_{rse} \end{pmatrix} \quad (4)$$

those position on the particle $\vec{r}_{rse} = r_p \cdot \vec{e}_{rse}$ can be obtained which reflect the laser beams on to the two detectors. According to the laws of geometrical optics, the incident rays are reflected at these positions with their specific local intensity on to the detectors.

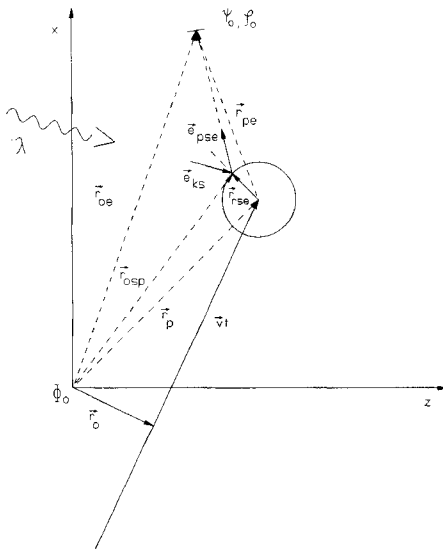


Fig. 2: Signal generation on the receiver.

The reflecting rays are not parallel and consequently interference at the detectors forms the measured signals. In this way the local intensities of both laser beams can be taken into account. The reflected rays have the following form [9]:

$$\vec{E}_{se} \sim \vec{E}_{pse} e^{-j(\vec{k}_{pse} \cdot \vec{r}_{pse} + \Phi_{pse} - \omega t)} \quad (5)$$

\vec{E}_{pse} is proportional to the intensity of the laser beam s at the point of reflection p relative to detector e . Φ_{pse} is the phase of the laser beam at the position of reflection. $\vec{k}_{pse} \cdot \vec{r}_{pse}$ gives the phase shift of the reflected ray between the point of reflection and the detector. By interference at the detector, the signal phase results from the difference in phase of the partial rays. Replacing \vec{r}_{pse} by $\vec{r}_{oe} - \vec{r}_p - \vec{r}_{rse}$ gives the phase of the signal [1] at detector 1:

$$\Phi_1 = \vec{k}_{p11} \vec{r}_{p11} - \vec{k}_{p21} \vec{r}_{p21} + \Phi_{p11} - \Phi_{p21} \quad (6a)$$

and at detector 2:

$$\Phi_2 = \vec{k}_{p12} \vec{r}_{p12} - \vec{k}_{p22} \vec{r}_{p22} + \Phi_{p12} - \Phi_{p22} \quad (6b)$$

The phase difference between the two detectors is given by

$$\Delta\Phi = \Phi_2 - \Phi_1 = \vec{k}_{p21} \vec{r}_{p21} + \vec{k}_{p12} \vec{r}_{p12} - \vec{k}_{p11} \vec{r}_{p11} - \vec{k}_{p22} \vec{r}_{p22} - \Phi_{p11} - \Phi_{p22} + \Phi_{p21} + \Phi_{p12} \quad (7)$$

Eq. (7) is universally valid. For a particle at the centre of the measurement volume and for nearly parallel vectors $\vec{r}_{01}, \vec{r}_{p11}, \vec{r}_{p21}$ and $\vec{r}_{02}, \vec{r}_{p22}, \vec{r}_{p12}$, the summand in Eq. (7) can be expressed by the position of the detectors. In this way the following well known relationship can be derived [4-7]:

$$\Delta\Phi = \sqrt{2^3} \pi \frac{d_p}{\lambda} \left(\sqrt{1 - \cos\psi_0 \cos\phi_0 \cos(\theta/2) - \sin\psi_0 \sin(\theta/2)} - \sqrt{1 - \cos\psi_0 \cos\phi_0 \cos(\theta/2) + \sin\psi_0 \sin(\theta/2)} \right) \quad (8)$$

A more exact result is obtained by taking into account the different directions of the reflected rays and the points of reflection on the sphere by iteration. Considering the detector position, the particle position and the points of reflection, the following more exact equation results:

$$\begin{aligned} \Delta\Phi = & \Phi_{p21} + \Phi_{p12} - \Phi_{p11} - \Phi_{p22} - (\vec{r}_{r11} - \vec{r}_{r12}) \vec{k}_1 - \\ & - (\vec{r}_{r22} - \vec{r}_{r21}) \vec{k}_2 - \frac{\pi}{\lambda} r_0 [(x_p + x_{r11})^2 + (y_p + y_{r11})^2 + \\ & + (z_p + z_{r11})^2 - (x_p + x_{r21})^2 - (y_p + y_{r21})^2 - \\ & - (z_p + z_{r21})^2 + (x_p + x_{r22})^2 + (y_p + y_{r22})^2 + \\ & + (z_p + z_{r22})^2 - (x_p + x_{r12})^2 - (y_p + y_{r12})^2 - (z_p + z_{r12})^2] \end{aligned} \quad (9)$$

The last summand in Eq. (9) can be ignored. It represents the influence of the different distances of the points of reflection to the detector and its change along the trajectory of the particle through the measurement volume. It describes the phase variation along the trajectory within a Doppler burst and may lead to erroneous particle sizes.

2 Phase Shift on Trajectories beyond the Beam Waist

The above approach can easily be adapted for use with non-plane wave-fronts. For this, in Eq. (4) the orientation of the wave-fronts has to be taken into account at the points of reflection and the newly derived points of reflection have to be used with the respective phase of the laser beam in Eq. (7). Both the orientation of the wave-fronts and the phase of the laser beam can be obtained by using the solution of the wave equation for a Gaussian-shaped laser beam by *Kogelnik and Li* [10] and *Davis* [11]. The electric field of the laser beam near the beam waist is given by [9]

$$\vec{E}^z(r_s, z_s) = E(0, 0) \frac{r_{os}}{r_{ms}} e^{-\left(\frac{r_s}{r_{ms}}\right)^2} e^{-j\left\{\frac{2\pi}{\lambda}\left(z_s + \frac{r_s^2}{2R_s}\right) - \arctan\left(\frac{\lambda z_s}{\pi r_{os}^2}\right) - \omega t\right\}} \quad (10)$$

The beam radius (Figure 3) is given by

$$r_{ms}^2 = r_{os}^2 \left[1 + \left(\frac{\lambda z_s}{\pi r_{os}^2} \right)^2 \right] \quad (11)$$

and the radius for the surface of equal phase is given by

$$R_s(z_s) = z_s \left[1 + \left(\frac{\pi r_{os}^2}{\lambda z_s} \right)^2 \right] = z_s \left[1 - \frac{z_{os}}{z_s} \right] \quad (12)$$

Accordingly, the phase at the points of reflection resulting from Eq. (10) is given by

$$\Phi_{pse} = \frac{2\pi}{\lambda} \left(z_s + \frac{r_s^2}{2R_s} \right) - \arctan \left(\frac{\lambda z_s}{\pi r_{os}^2} \right). \quad (13)$$

In Eqs. (10)-(13) a beam coordinate system is used (Figure 3). In order to use these equations in phase Doppler anemometry, the coordinates of the reflection points have to be converted to the central coordinate system (Figure 1) [9]:

$$\vec{r}(x_s, y_s, z_s) = \begin{vmatrix} x_s \\ y_s \\ z_s \end{vmatrix} = \begin{vmatrix} x \cos(\theta/2) - z \sin(\pm \theta/2) \\ y \\ x \sin(\pm \theta/2) + z \cos(\theta/2) \end{vmatrix}. \quad (14)$$

The coordinates x, y, z have to be replaced by the points of reflection on the particle:

$$\vec{r}_{osp} = \begin{vmatrix} x_p + x_{rse} \\ y_p + y_{rse} \\ z_p + z_{rse} \end{vmatrix}. \quad (15)$$

The vector of the phase front in the centre of the particle (Figure 3) is obtained from Eqs. (12) and (14):

$$\vec{R}_s(x_s, y_s, z_s) = [\vec{i}x_s + \vec{j}y_s + \vec{k}(z_s - z_{os})] \cdot \text{Sgn}(z_s). \quad (16)$$

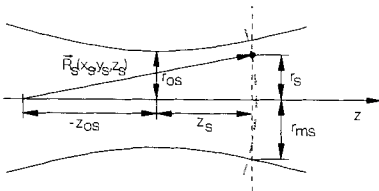


Fig. 3: Phase front within a laser beam.

The orientation of the incident ray at the points of reflection is given by

$$\vec{e}_{ks} = \frac{\vec{R}_s(x_s, y_s, z_s)}{|\vec{R}_s(x_s, y_s, z_s)|}. \quad (17)$$

The position of the points of reflection can be computed iteratively for every position of the particle within the laser beam by using Eqs. (11)-(17) and the law of reflection (Eq. (4)). The phase difference of the burst signals detected by the two detectors corresponds to the measured time lag of the burst if the phase shift within a burst is ignored. The time lag for every particle position can be computed from the points of reflection [1] using

$$\Delta t = \frac{1}{2v_x} [- (x_{r11} + x_{r21} - x_{r22} - x_{r12}) + (z_{r11} - z_{r21} + z_{r22} - z_{r12}) \tan(\theta/2)]. \quad (18)$$

If the wave-fronts are considered plane and the vectors $\vec{r}_{01}, \vec{r}_{p11}, \vec{r}_{p21}$ and $\vec{r}_{02}, \vec{r}_{p22}, \vec{r}_{p12}$ are parallel, the following equation is derived:

$$\Delta t = \frac{d_p}{\sqrt{2}^3 v_x} \left\{ \frac{\sin \psi_0 - \cos \psi_0 \cos \varphi_0 \tan(\theta/2)}{\sqrt{1 - \cos \psi_0 \cos \varphi_0 \cos(\theta/2) - \sin \psi_0 \sin(\theta/2)}} + \frac{\sin \psi_0 + \cos \psi_0 \cos \varphi_0 \tan(\theta/2)}{\sqrt{1 - \cos \psi_0 \cos \varphi_0 \cos(\theta/2) + \sin \psi_0 \sin(\theta/2)}} \right\}. \quad (19)$$

Eq. (18) is also valid for particle positions outside the beam waist if the coordinates of the points of reflection are computed iteratively for non-plane wave-fronts.

3 Simulation Results

Systematic errors of PDA in the reflective mode can be analysed by using the approach described above. As the trajectory of the particles through the measurement volume is usually not known, simulations are done by computing the trajectory-dependent phase difference for a fixed particle diameter according to Eqs. (9) and (18) and analysing them (that is, computing the particle diameter that would be measured) with Eqs. (8) and (19) valid for plane wave-fronts.

Next the influence of the measurement volume on the measured particle size is computed. A stream of single-sized particles is assumed to move in a laminar flow along the x -axis. Taking this into account, the particle size which would be measured results in a particle size distribution. For the example result to be presented next, the particle diameter is assumed to be $d_p = 10 \mu\text{m}$. The off-axis-angle φ is 150° and the elevation angle ψ is 10° . The detectors are situated at a distance, r_0 , of 200 mm from the centre of the measured volume.

The radius of the beam waist r_{os} is $15 \mu\text{m}$. The angle of intersection of the laser beam is varied with this investigation. First the influence of the position of the particle trajectory on the resultant phase difference is computed. Figure 4 gives the change of the phase difference with varying particle position on the x -axis. The position of the trajectory is $y_0 = 0 \mu\text{m}$ and different z_0 coordinates are considered.

The change of the phase difference results from the divergence of the laser beams, which gives a changing Doppler frequency within a Doppler burst. It also results from the non-symmetric position of the particle in relation to the detectors. This results in only small changes of the phase difference, and its influence is therefore not considered important for phase Doppler

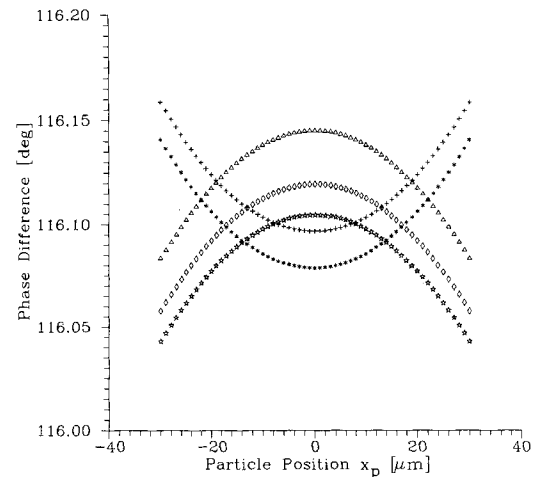


Fig. 4: Phase variation within a Doppler burst for a particle trajectory with $x_0 = 0, y_0 = 0, \Theta = 10^\circ, (\Delta) z_0 = -20 \mu\text{m}; (\diamond) z_0 = -10 \mu\text{m}; (\star) z_0 = 0 \mu\text{m}; (+) z_0 = 10 \mu\text{m}; (*) z_0 = 20 \mu\text{m}$.

anemometry. The greatest value of the phase difference error is about 10^{-3} degrees.

More important errors result if the trajectory of the particle is not on the x -axis. Figure 5 gives the results if the z_0 -position of the trajectory is changed. Two different beam intersection angles have been used for the simulation. The same phase difference is obtained from Eq. (9), which takes the non-plane wave-fronts into account and from the phase differences computed from $\omega_D \Delta t$ where the time lag Δt is obtained by using Eq. (18). This result is important for calculating the particle size from phase differences greater than 2π with only two detectors by using the cross-correlation method described in Ref. [1]. For small beam intersection angles (e. g. $\Theta = 5^\circ$) there is no difference between the phase difference computed for plane wave-fronts from Eqs. (8) and (9) and the results from Eq. (18) for non-plane wave-fronts.

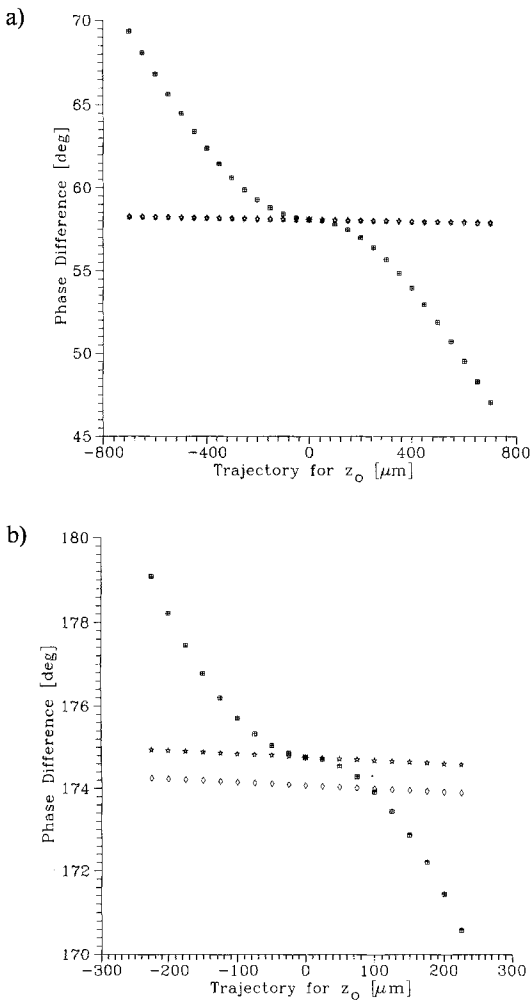


Fig. 5: Phase difference between the Doppler signals as a function of the z_0 trajectory coordinate for $x_0 = 0, y_0 = 0$. (a) $\Theta = 5^\circ$; (b) $\Theta = 15^\circ$. (\diamond) Eq. (8); ($*$) Eq. (19); (∇) $\omega_D \Delta t$, Eq. (18) for plane wave-fronts; ($+$) Eq. (9) for non-plane wavefronts; (\square) $\omega_D \Delta t$, Eq. (18) for non-plane wave-fronts.

With greater beam intersection angles (e. g. $\Theta = 15^\circ$) the phase difference according to Eq. (8) is about 0.5% in error from the exact results. The results have been plotted for a trajectory variation twice the defined measurement volume in the z -direction ($\Theta = 5^\circ, c = 343 \mu\text{m}$; $\Theta = 15^\circ, c = 114 \mu\text{m}$). As can be seen, they are not the same for the two beam intersection angles, because the z -size of the measurement or detection volume is

dependent on the beam intersection angle for a constant beam divergence. The greater the intersection angle, the shorter is the z -dimension of the measurement volume. While a beam intersection angle of $\Theta = 5^\circ$ leads to a maximum phase difference error of $\pm 18\%$ in this z -range, for $\Theta = 15^\circ$ the phase difference error is only about $\pm 2\%$.

Next, the influence of the beam divergence on the time lag is investigated by changing the wavelength for a constant size of the measurement volume. Figure 6 demonstrates that the error increases with increasing divergence angle.

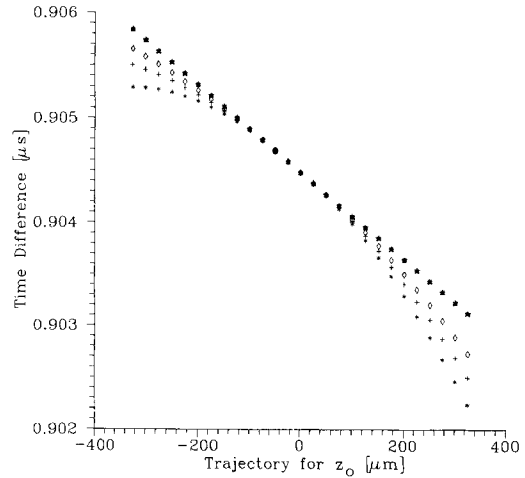


Fig. 6: Time displacement between the Doppler signals according to Eq. (18) as a function of the z_0 coordinate for $x_0 = 0 \mu\text{m}, y_0 = 0 \mu\text{m}$ and different wavelengths. Eq. (19): (Δ) 488 nm; (∇) 633 nm; (\times) 780 nm. Eq. (18) for non-plane wave-fronts: (\diamond) 488 nm; ($+$) 633 nm; ($*$) 780 nm.

The results of shifting the trajectory in y_0 given in Figure 7 are noteworthy. The off-axis angle φ changes with the y_0 -position of the trajectory because the detectors are positioned non-symmetrically with respect to the x - y plane. The curve phase difference versus y_0 -position is therefore also non-symmetric. The phase difference computed from the time lag gives a linear relationship. The cause of the non-linear relationship according to Eq. (9) is apparently local changes of the phase within the laser beam.

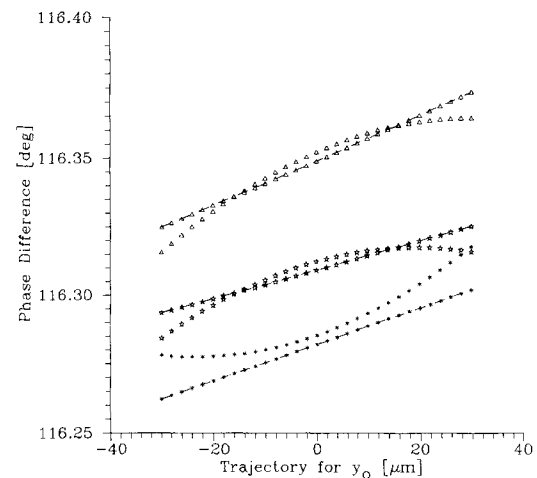


Fig. 7: Phase difference as a function of the y_0 trajectory coordinate for $x_0 = 0 \mu\text{m}, z_0 = 0 \mu\text{m}, \Theta = 10^\circ$. Phase from the time displacement with $-$, phase according to Eq. (9) without $-$, (Δ) $z_0 = -20 \mu\text{m}$; (∇) $z_0 = 0 \mu\text{m}$; ($*$) $z_0 = 20 \mu\text{m}$.

Figure 8 shows the influence of trajectories which are inclined to the x - y -plane. In this case particle sizes were computed from the resultant phase differences by using Eq. (8). As can be seen, the particle size error increases with greater inclination and a greater beam intersection angle.

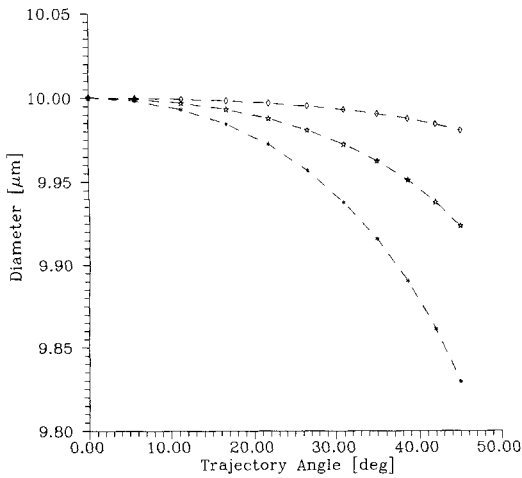


Fig. 8: Particle diameter according to Eq. (8) as a function of the angle between particle trajectory and x -axis for $x_0 = 0 \mu\text{m}$, $y = 0 \mu\text{m}$, $z_0 = 0 \mu\text{m}$. (\diamond) $\Theta = 5^\circ$; (\star) $\Theta = 10^\circ$; (\ast) $\Theta = 15^\circ$.

Problems which have been analysed separately above are encountered together in a real flow. Therefore, a particle flow of monodisperse diameters results in a statistical particle size distribution depending on the specific influence of the measurement volume. To show this influence, in the following the expected particle size distribution is computed for a particle flow with monodisperse diameters and the expected error in measuring the mass flux is determined.

Two optical set-ups having the same beam waist diameter $2r_{os} = 30 \mu\text{m}$ but different beam intersection angles of $\Theta = 5^\circ$ or $\Theta = 15^\circ$ were investigated. The results are plotted in Figure 9. To show the influence of the measurement volume, particle size distributions were computed for a laminar flow in the direction of the x -axis. The number of particles was 5000 and the sampling volume was 1.5 times the measurement volume defined by the e^{-2} intensity reduction of the measurement volume. The size distribution was computed with phase shift measurements using diameter computation according to Eq. (8), and then with time lag measurements using the following diameter

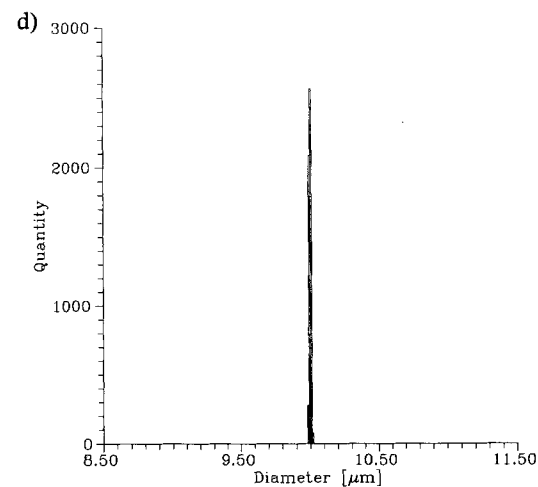
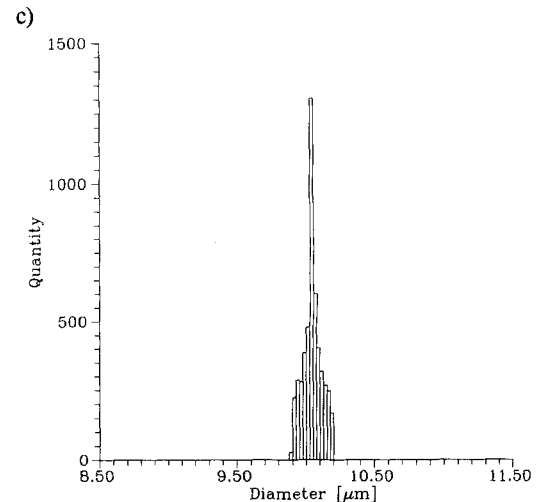
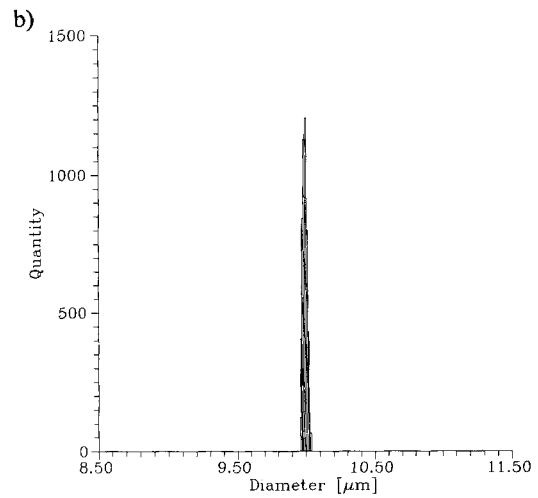
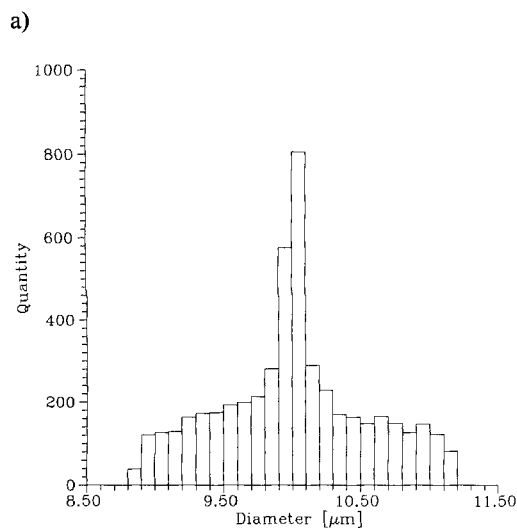


Fig. 9: Size distribution evaluated from: (a) phase difference according to Eq. (8), $\Theta = 5^\circ$; (b) time displacement according to Eq. (19), $\Theta = 5^\circ$; (c) phase displacement according to Eq. (8), $\Theta = 15^\circ$; (d) time displacement according to Eq. (19), $\Theta = 15^\circ$.

evaluation according to Eq. (19). The size distributions become smaller with increasing beam intersection angles because the sampling volume is decreasing. The beam divergence is independent of the beam intersection angle. The results of phase difference evaluation are given in Figure 9a and c.

With a beam intersection angle of $\Theta = 5^\circ$ the mean diameter \bar{d}_p is $10.00508 \mu\text{m}$ and with a beam intersection angle of 15° \bar{d}_p is $10.04363 \mu\text{m}$. This increase in error for a greater Θ is caused

by the difference between the results according to Eq. (8) and the more exact results according to Eqs. (9) and (18) (Figure 5b). The corresponding error in mass flow in $\Delta m/m = 1\%$ with $\Theta = 5^\circ$ and $\Delta m/m = 1.3\%$ with $\Theta = 15^\circ$.

The results from evaluating the time lag are shown in Figure 9b and d. This distribution is thinner. The time lag is the ratio of phase shift to Doppler frequency. Phase shift and Doppler frequency both depend on the curvature of the phase front of the laser beam. Therefore, the time lag method gives a more exact result. There is virtually no difference between the mean diameter of the size distribution and the real diameter of the particle. With $\Theta = 5^\circ$ the mean diameter \bar{d}_p is $9.99969 \mu\text{m}$ and with $\Theta = 15^\circ$ \bar{d}_p is $9.99971 \mu\text{m}$. In both cases the error in mass flux is about $\Delta m/m = -0.1\%$. For measuring the particle diameter, phase difference evaluation gives good results, but for measuring mass flux, time lag evaluation gives more exact results.

Measuring the time lag $\Delta t = \Delta\Phi/\omega_D$ is not difficult because both phase shift $\Delta\Phi$ and Doppler frequency ω_D are normally measured. This method is therefore recommended. Additionally with this method there is also in principle no uncertainty with a restricted size range as with the phase difference method for a phase difference $> 2\pi$ [1].

4 Conclusion

For PDA operating in the reflective mode the influence of the Gaussian intensity distribution of the laser beam and the curvature of the phase fronts on the measured PDA signals was computed using geometrical optics. Evaluation of the particle diameter from the phase difference and also from the time lag was investigated.

Both methods result in a statistical particle size distribution. Bias and standard deviation are reduced with the time lag method. The error of the phase difference method is especially pronounced when considering mass flow rates. Application of the time lag method is recommended.

The theory applied is restricted to the validity of geometrical optics and to dominant reflected light detection. This means that the particle diameter should be much larger than the laser wavelength.

5 Symbols and Abbreviations

A	amplitude
a	half-axis of the measurement volume in the x-direction
d	diameter
E	electric field strength
e	unit vector
k	wave vector
m	mass
LDA	laser Doppler anemometry
PDA	phase Doppler anemometry

r	radius, distance
t	time
v	velocity
x, y, z	global cartesian coordinates

Greek symbols

Θ	intersection angle of the laser beams
λ	wavelength
Φ	phase
φ	off-axis angle
ψ	elevation angle
ω	circular frequency

Subscripts

D	Doppler
e	receiver
o	origin
p	particle
r	radius
s	beam
x, y, z	coordinates

Additional Definitions for any Symbol or Function x :

\vec{x}	vector
\bar{x}	mean value
$x_{x, y, z}$	value in coordinate direction or related to it
$x_1, 2, \dots$	index for direction or number distinction
Δx	difference, deviation, error
x^{\wedge}	complex value

6 References

- [1] H. E. Albrecht, M. Borys, K. Hübner: Generalized Theory for the Simultaneous Measurement of Particle Size and Velocity Using Laser Doppler and Laser Two-Focus Methods. Part. Part. Syst. Charact. 10 (1993) 138-145.
- [2] N. E. Tayali, C. J. Bates: Particle Sizing Techniques in Multiphase Flows: A Review. Flow Meas. Instrum. 1 (1990) 77-105.
- [3] F. Dust, M. Zaré: Laser Doppler Measurements in Two Phase Flows. Proc. LDA Symp. Copenhagen (1975) 403-429.
- [4] M. Saffman, P. Buchhave, H. Tanger: Simultaneous Measurement of Size, Concentration and Velocity of Spherical Particles by a Laser Doppler Method. Proc. 2nd Int. Symp. on Laser Anemometry to Fluid Mechanics, Lisbon (1984).
- [5] M. Saffman: Optical Particle Sizing Using the Phase of LDA-Signals. DANTEC Information 5 (1987) 8-13.
- [6] W. D. Bachalo: Method for Measuring the Size and Velocity of Spheres by Dualbeam Light-scatter Interferometry. Appl. Opt. 19 (1980) 363-369.
- [7] K. Bauckhage, H. H. Flögel: Correlation of Simultaneously Measured Droplet Sizes and Velocities in Nozzle Sprays. Part. Charact. 1 (1984) 112-116.
- [8] F. Durst, W. H. Stevenson: Influence of Gaussian Beam Properties on Laser Doppler Signals. Appl. Opt. 18 (1979) 516-524.
- [9] H. E. Albrecht: Laser-Doppler-Strömungsmessung. Akademie-Verlag, Berlin 1986.
- [10] H. Kogelnik, T. Li: Laser Beams and Resonators. Appl. Opt. 10 (1966) 1550-1567.
- [11] L. W. Davis: Theory of Electromagnetic Beams. Phys. Rev. 19 (1979) 1177-1179.